Contents

1 Introduction

The feedback control of a robotic gymnast attempt to model a gymnast swinging from the hanging position to the inverted balancing position on a bar as a double pendulum connected with a hinge. The lower pendulum in the stable equilibrium position is actuated by a motor to model the behaviour of the swinging legs. This system describe in the mathematical sense lends itself to be a underactuated system. Underactuated systems are where the control input cannot command an instantaneous acceleration in any direction of the state variables describing the system. The robotic gymnast needs to use the coupling between the actuated pendulum and unactuated pendulum to swing and balance the gymnast from it's stable equilibrium position to the unstable equilibrium position [1].

The field of underactuated robotics are becoming increasingly more important due to multiple fields such as the rocket,satellite,aerospace and the consumer products relying more on control systems which needs to control a underactuated system. Examples such as the James Webb Telescope for the satellite industries, SpaceX landing of their rockets, and drones for consumers products are easily media attention seekers that are underactuated systems.

The double pendulum that consist of a swing-up and balancing parts, is a underactuated problem, that employs fundamental concepts which exist in most underactuated problems. An complex non-linear problem of the swing-up part and the well defined linearised system of balancing the inverted double pendulum. The double pendulum is a great introductory problem to solve to step into the world of underactuated robotics.

The process of achieving the swing up and balance of the robotic gymnast consist of a sequence of steps that is critical to the success of the project. The project starts of by doing a literature study to learn and understand new concepts and the design paradigms towards the characteristic properties of a underactuated system. The literature study equips the reader to solve problems by understanding the fundamental behaviour of the system. Simulation of the system is done to verify the newly learned concepts, learn the impact of system properties on system behaviour and test different design paradigms. This will entail the use of information technology and engineering tools to implement the system on a simulation package and make use of scientific and engineering knowledge to distinguish between conflicting and authentic behaviour describe by models and supported by the literature study. The

mechanical design of the system is to follow based on the requirements and specification determined during simulation and to verify the accuracy of the model. The electronic design will occur simultaneously to measure the state variables and perform signal conditioning allowing the control system to be implemented. These designs will require the synthesis of components, system and procedural design. The project will come to life by integrating the mechanical and electronic designs to allow the verification of the experimental data with simulation data. Problem solving and the application of engineering knowledge will be key to identify and verify any hypothesis in behaviour of the system. Reporting on the project will occur during the various phases described above and will demonstrate the competence to communicate effectively in writing. The project will be supervised by a researcher who will give critical feedback on the student's performance and project task. The relationship will illustrate the individual, team and multidisciplinary working during the project.

This report will document the process as describe in the preceding paragraph. The first chapter will provide a review of the essential concepts in control theory. This will be followed by the model describing the robotic gymnast and the assumptions made during the derivation of the model. Next the report describe the design paradigms to solving the non-linear swing-up of the gymnast. The report then describe the balancing of the gymnast in the unstable equilibrium position. Next the report discuss how the transition between the non-linear swing-up and the linearised will function.

2 Review of Fundamental Concepts

3 Derivation of Double Pendulum

The robotic gymnast is modeled as two pendulums connected together with a hinge. Each pendulum is modeled as having their mass distributed arbitrary along their axis and a torque actuating the lower pendulum. Friction is modeled as proportional to the angular velocity of the pendulums. The friction that develops at the hinge connecting the 2 pendulums are a function of the relative motion between the two pendulums. The angle, ϕ was purposefully chosen relative to angle, θ. Figure 1 displays the free body diagram of the robotic gymnast.

Deriving the equation of motion of the robotic gymnast can be approached on different methods, but by exploring the system it can be shown that the
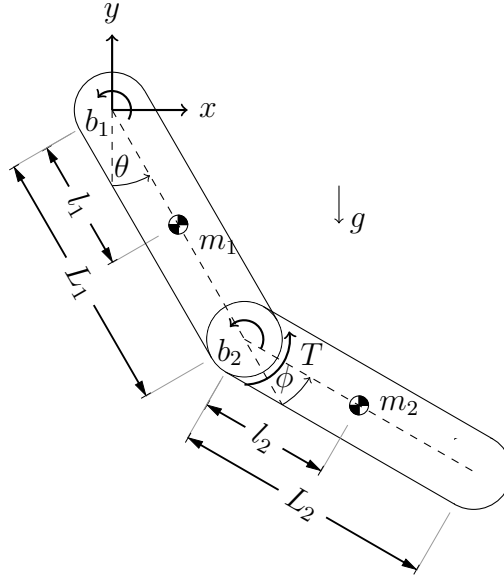
Figure 1: Free Body Diagram of the Double Pendulum

system's energy is easily defined. The energy in the system are the potential energy of the 2 pendulums, the rotational kinetic energy of the underactuated pendulum and the velocity- and rotational kinetic energy of the actuated pendulum. The system's energy is easily defined and for this reason the Lagrange-Euler equation is used to derive the differential equation describing the system dynamics. The derivation of the differential equation can be found in Appendix A.

The equation of motion for the robotic gymnast is non-linear. It contains terms that is a function of squared angular velocity, sine and more. These non-linearity can be linearised around a working point, but during the swing-up of the robotic gymnast, where the gymnast will operate in a large operating region linearisation will cause dramatic errors and thus these non-linearities need to be taken into account. How to overcome these non-linearities is discussed in the following section.

4   Swing Up of the Double Pendulum

It has been shown that it is not possible to linearise the dynamics of the gymnast by means of static state feedback and non-linear transformation [2], but it is possible to achieve a linear response from one of the state variables by implementing a non-linear feedback. This non-linear feedback is the par-

5

tial feedback linearisation, where any of the 2 responses of the state variables can be linearised.

Collocated linearisation of the non-linear model is done to linearise the response of the actuated pendulum resulting in being proportional to the input of the system. The derivation of the collocated linearisation is shown in appendix C. This input can be selected to force the actuated pendulum to follow a desired trajectory [3].

To force the actuated pendulum to follow a desired trajectory, it is possible to pump energy into the system. The desired trajectory for ϕ^d is chosen as

$$\phi^d = \alpha \arctan(\dot{\theta})$$

[3]. The α coefficient constrains the actuated pendulum to stay within a interval of $\phi \in [-\alpha, \alpha]$ [3]. This provides better control over the system to stay within the null controllability region when the system reaches the unstable inverted position to switch over to the linearised model.

5 Balancing of the Double Pendulum

The balancing of the gymnast will be achieved by catching the gymnast when the swing-up control algorithm has brought the gymnast to the null controllability region. The null controllability region is the set of states that can be steered to inverted unstable equilibrium position in a fixed time with a constrained control input [4].

Within the null controllability region the gymnast can be approximated as a linear system. Linearising the model at

$$\vec{Q}_s = [\vec{q}_s, \dot{\vec{q}}_s, \ddot{\vec{q}}_s]^T = [\pi, 0, 0, 0, 0, 0]$$

the unstable inverted equilibrium position using the Taylor Series Expansion the model can be written in the state space form. The linearisation of the gymnast model is shown in Appendix B. The state space variables are chosen as Δq and $\Delta \dot{q}$ which results in the state space representation as:

$$\dot{\vec{x}} = \boldsymbol{A}\vec{x} + \boldsymbol{B}u$$

and

$$\vec{y} = \boldsymbol{D}\vec{x} + \boldsymbol{0}u$$

.

When the linearised system is at rest, any disturbance will result in a theoretically infinite growth of the state variables, but this behaviour can be controlled by introducing feedback. The instability of the system can be identified by examining the poles of the systems. The linearised model contains 4 real, 2 positive and 2 negative poles, and these poles will be moved to the desired position by using the method of dominant poles. The method of dominate poles chooses a pair of the poles for the closed-loop system and select the other open-loop poles to have real parts. This allows the higher-order system response to be characterised as a second-order response [5]. The linearised model already has 2 negative real poles which is chosen to stay the same. The real positive poles were selected based on the following specifications.

These specification was selected on increasing the null controllability region with a low settling time. Due the approximation of the linearised model the null controllability region may be larger than the derived sized [6].

6 Null Controllability Region

The null controllability region is the set of states, $\vec{x_0} \in \Re$ which can be steered with a constrained input in finite time to the origin. This region is important because it provides the boundary where the linear controller is capable of catching the swinging gymnast. The possibility exist that the set might be larger due to approximation in the working point during linearisation of the system [6].

To determine the null controllability region requires a transformation into independent equation and followed by a technique describe in .. . The linearised system are coupled and due to damping effect results in a quadratic eigenvalue problem. The de-coupling can be done by using phase-synchronisation describe in [7] and shown in Appendix XXX. The phase-synchronisation results in 2 transformed eigenvalues, λ' and creates 2 damping ratio's, ζ' to from two independent second-order equations. The values for λ''s and ζ''s is as follows:

$$\boldsymbol{\lambda} = []^T$$

$$\boldsymbol{\zeta} = []^T$$

From these two independent second-order equations the null controllability region can be determine using time-reversal describe in [4].

$$\vec{x} = e^{\boldsymbol{A}t}\vec{x_0} + \int_{t_1}^{t_2} e^{-\boldsymbol{A}t}\boldsymbol{B}udt$$

$$\mathcal{R} = - \int_{-\infty}^{0} e^{A\tau} b \, sgn(c' e^{A\tau}) d\tau$$

$$\mathcal{C}$$

7 System Identification

The system identification tests are done to determine the characteristics that describe the behavior of the system. These characteristics include the damping ratio's and natural frequencies of the system around the unstable equilibrium position. The system are describe by 2 independent parameters, θ and ϕ which defines the position of the non-actuated and actuated pendulums. The system is thus a 2 degree of freedom (2DOF) system and it is expected to contain 2 natural frequencies each accompanied by a damping coefficient.

The first natural frequency of the system is determine by inspecting the response of the system when starting at a initial condition and keeping $\phi = 0$ rad constant throughout the response. This was done by using a lightweight PVC pipe that has negligible effect on the weight of the system. The actuated pendulum and non-actuated pendulum are constrained to this pipe to ensure the 2 pendulums stay in-line with each other and thus ensuring $\phi = 0$ rad. The response of the system is shown in Figure 3 starting at a initial condition of roughly $\theta = \frac{\pi}{2}$. The accuracy of the initial conditions is of little importance, but the initial condition must allow the response to contain a few oscillation to accurately determine the parameters of interest. The second natural frequency is determined by analysing the response of the system when ϕ starts at a initial condition and keeping $\theta = 0$ rad throughout the response. This was accomplished by constraining the non-actuated pendulum using hard stops. Figure 4 shows the measured response of the system when ϕ starts at a initial condition and keeping θ constant.ith with an approximated response that is determined by the parameters shown in Table **??**.

The natural frequencies of the system is identified by inspecting the frequency content of the time-domain responses. The frequency content of the initial condition responses of both experiments are shown in Figure 2, by applying the Fast Fourier Transform (FFT) algorithm to the time-domain signals. The FFT indicates the natural frequencies by the predominant peaks across the frequency spectrum which are tabulated in Table 1.

The responses shown in Figure 3 and 4 are decaying with time and this

decaying behaviour can be modeled by the following equation:

$$\tau(t) = -\zeta\omega_n t$$

Where ω_n is the natural frequency of the system and ζ the damping ratio of the system. The natural frequencies of the system has already been determined and thus linear regression can be used to determine the best ζ that will fit the measured data. The decaying functions are shown in Figure 3 and 4 with the best fit ζ values shown in Table 1. It is visible from the responses that the damping ratio changes when the response are near steady state. These new damping ratio's are also tabulated in Table 1 and shown in Figure 3 and 4.

The input to the system is the torque delivered by the motor and the magnitude and direction is determined by the control laws. The model describing the system in (1) assumes the torque delivered to the system is instantaneously available. This is inaccurate due to the DC motor model describing the torque delivered by the model when applying a DC voltage. The input that the motor will be receiving is a Pulse-Width-Modulated (PWM) signal to represent a DC voltage.

Experiments are done to determine the relationship of between the duty-cycle of the PWM signal and the torque provided by the motor. These experiments are done by incrementing the duty-cycle of the PWM signal that the motor receives when the shaft is kept fix against a hardstop. The motor-driver that controls the motor has a feedback pin that provides a proportional current of $\frac{1}{375}$ of the current flowing through the motor. This proportional current is allowed to flow through a known resistor. The voltage across the resistor is measured and provides a indication of the current flowing through the motor. The mean value of the voltage measured on the oscilloscope is taken and mapped backwards to determine the current. Figure 5 shows the measured data with a line of best fit. It is clear that there exist a linear relationship between the duty-cycle of the PWM signal and the torque the motor can provide.

Figure 3 shows the decaying function with properties that are shown in Table ?? and it is visible that the calculated values provides a acceptable approximation of the measured data.

8   Simulating the Double Pendulum

The process of simulating the robotic gymnast and ensuring the simulation provide a true representation of the system is discussed. Simulation of the robotic gymnast plays a important role during the design process. It allows

System Characteristic	Value	Mean	Standard Deviation
f_1	2 Hz		
f_2	3.9 Hz		
ζ_{11}			
ζ_{21}			
ζ_{12}			
ζ_{22}			

Table 1: System Characteristic & their Statistical Properties from 10 Experiments

the designer to develop a intuition for the system, enables the verification of dynamics and the creation of specification for the mechanical design. It will be presented by discussing how the simulation is a true representation of the system, how design specifications were determined and the influence of these parameters.

Simulation of the gymnast was done using MATLAB Simulink. The differential equations were implemented shown in (1) and non-linearities such as saturation of the motor, gearbox backlash and quantisation of sensory data were implemented to represent a true system. Verification of successful implementation of the differential equations were done by removing all non-linearities created by hardware and removing the damping effects. When the system is given a initial condition it is expected that the mechanical energy in the system will remain constant. This behaviour is shown in Figure **??** and verifies the correct implementation of the mathematical model.

System characteristic values such as inertia and pendulum lengths were unavailable during simulations owning to the mechanical design that was incomplete. Initially the system variables such as inertia and pendulum lengths were selected from values that represent a physical system. The accuracy of these values were credible being taken from a previous physical model. From these simulation motor specification could be determine and the influence of system variables could be analysed. Damping coefficients were chosen at random and the influence on the behaviour of the system was analaysed. (Describe how they influence the behaviour of the system).

Once the mechanical system was designed and manufactured and the system identification was completed the true system parameters could be used in the simulation. These system parameters are shown in Table 2. Using the system parameters shown in Table 2 the natural frequencies of the linearised system, the feedback gain matrix for the balancing control and the gain constants for the swing-up control were determined.
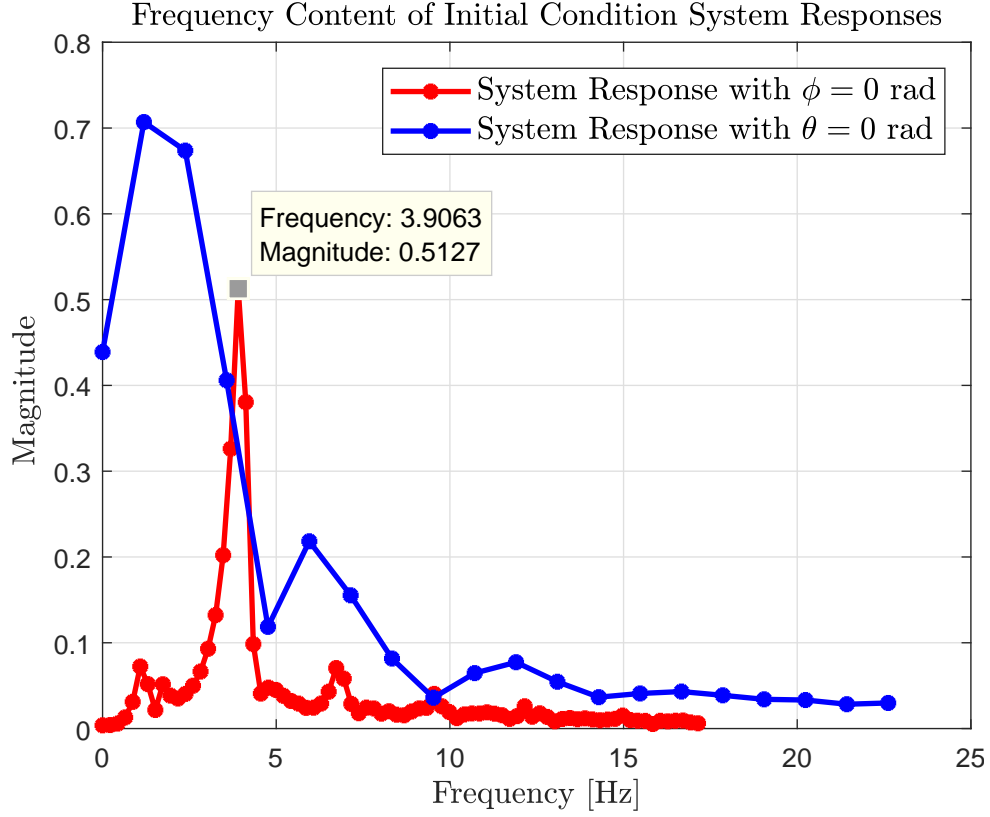
Figure 2: Frequency Content of Time-Domain Initial Condition Responses

Figure **??** shows the simulated swing-up and balance of the double pendulum. As discussed in the Swing-up Controller section the α value controls the relative angle between actuated pendulum and the non-actuated pendulum. This α value is decreased throughout the swing-up of the robotic gymnast to ensure the robotic gymnast can be approximated as a single pendulum to allow the linear controller to catch the swinging pendulums.

Figure **??** shows the response of the system when given a initial condition that is within the region of controllability in which the balancing controller moves the system to the unstable equilibrium position. The response shows that the balancing controller is capable of balancing the robotic gymnast when (elaborate more on specification,)

8.1   Feedback Control for Balancing Controller

The balancing controller is responsible for catching the swinging pendulums and let the system rest at it's unstable equilibrium position. The balancing
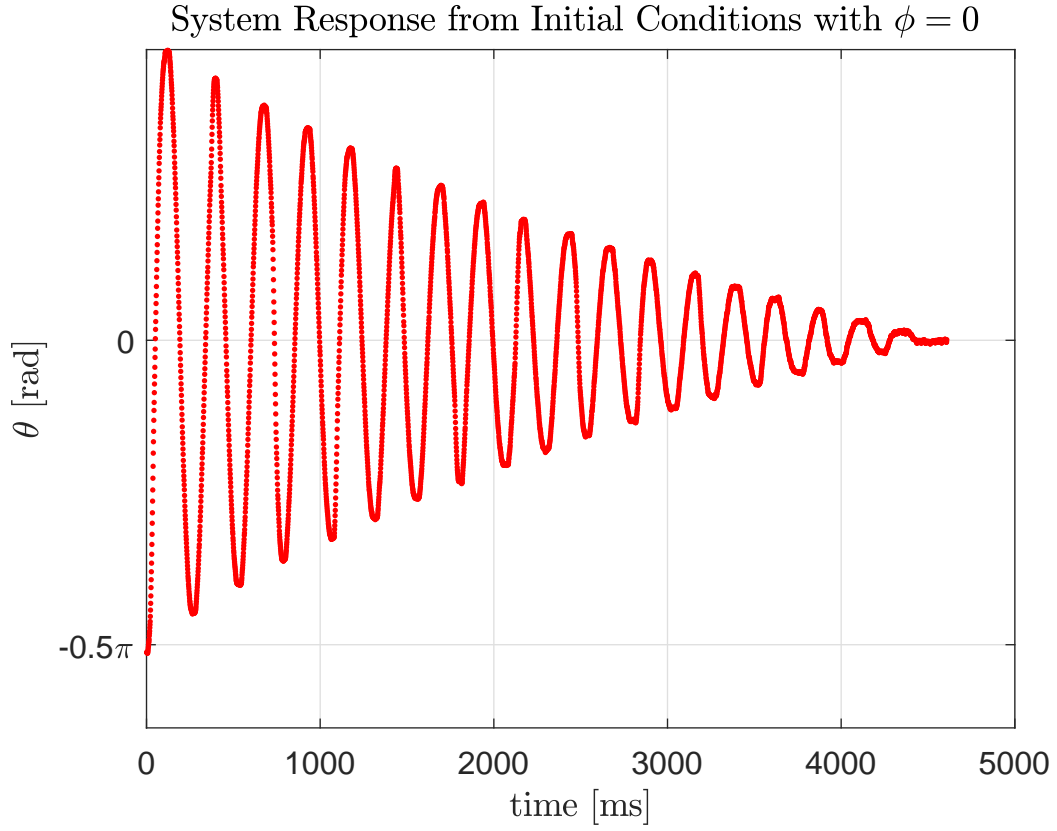
Figure 3: Initial Condition System Response while $\phi = 0\,\mathrm{rad}$

controller is thus required to take the system from a initial condition in the vicinity of the unstable equilibrium position and reach a steady state of balancing in the unstable equilibrium position.

The system will have unstable poles when in the vicinity of the unstable equilibrium position as shown in Table **??**. The feedback gain matrix must move these poles to a stable location with desired system response properties.

The desired system response

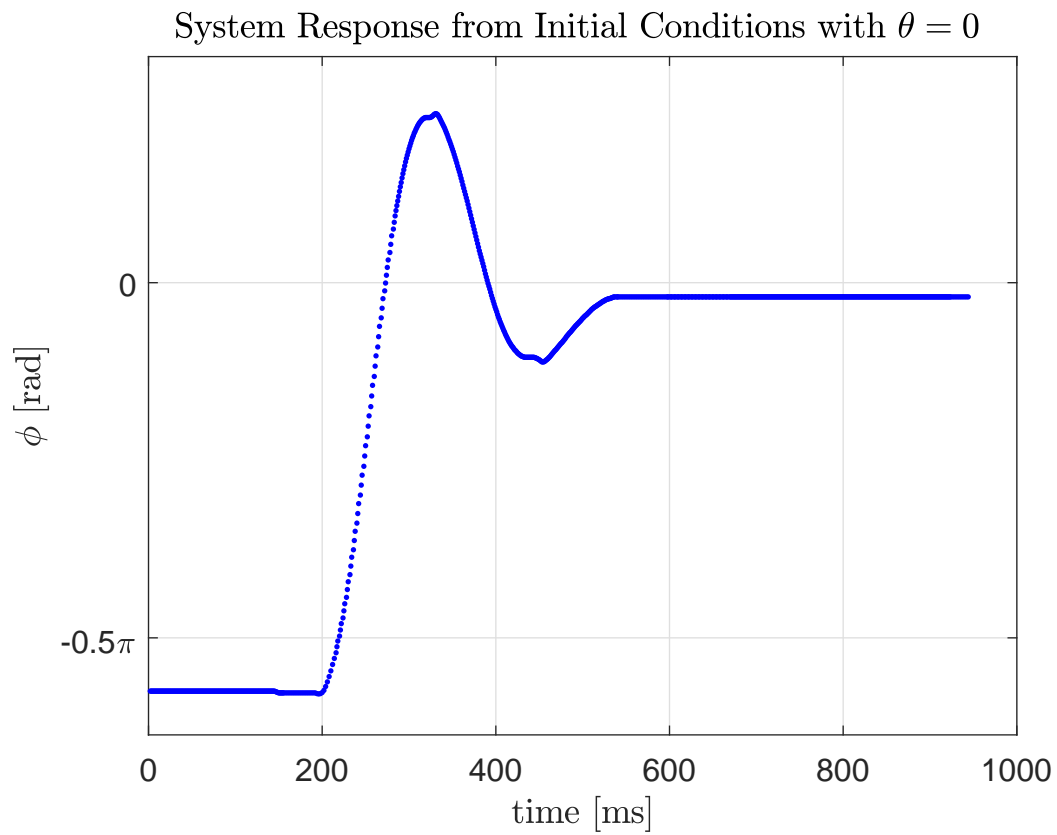System Response from Initial Conditions with $\theta = 0$

Figure 4: Initial Condition System Response while $\theta = 0\,\text{rad}$

8.2 Feedback Control for Swing-up Controller

9 Why Designing in the Continuous Time Domain is Sufficient
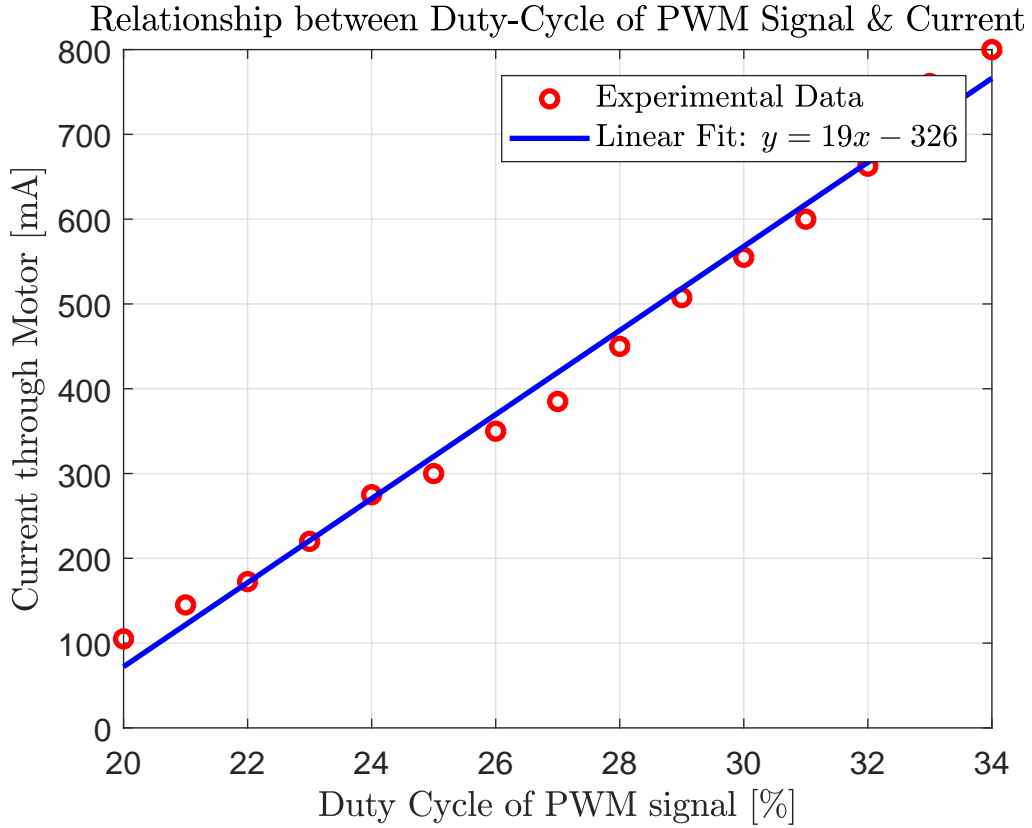
10 Mechanical Design of the Double Pendulum

Figure 5: Relationship between Duty-Cycle of PWM Signal and Current through Motor

11   Electronic Design of the Double Pendulum

11.1   System Description

Figure 6 provides/yields a system overview and how the different parts functions together. The micro-controller receives the different signals that has been correctly conditioned from supporting circuitry to interpret the dynamics of the system. From the observed condition it is able to output the correct signals to instruct the next command.

The digital logic circuit that consist of logic level converters acquires the signal from the micro-controller and performs signal conditioning to interface with the motor driver and determines the correct direction to rotate the motor.

The motor driver controls the DC brushed motor based of the digital

System Parameter	Value
L_1	$2\,\mathrm{m}$
L_2	$3.9\,\mathrm{m}$
I_A	$2\,\mathrm{kg}\cdot\mathrm{m}^3$
I_B	$2\,\mathrm{kg}\cdot\mathrm{m}^3$
m_1	$2\,\mathrm{kg}$
m_2	$2\,\mathrm{kg}$
l_1	$2\,\mathrm{m}$
l_2	$2\,\mathrm{m}$

Table 2: System Parameters

Component	Supply Voltage [V]
Digital Logic Components	5
μController	3.3
Motor Driver	12

Table 3: Suppy Voltage's for the different components

signals and provides a proportional feedback current that is fed/deliver to buffer.

The motor contains a encoder that indicates the direction and position of the rotor through digital signals that is sent through a digital logic filter to retrieve only critical information from the encoder signals.

The physical model contains a potentiometer that measures the non-actuated pendulums angle and is sent to the buffer.

The microcontroller will use the UART interface as it's data acquisition protocol to send the necessary information to the computer.

The micro-controller is programmed using the Serial Wire Debug (SWD) protocol to transfer the binaries from the computer.

Power is provided using a external 12V power-supply, which will power the motor, but also using a regulator to down convert/step to a 5V and 3.3V to power the microcontoller and the other peripherals.

11.2 Voltage Regulation

The various components require different supply voltages in the electronic design. The diffenrent supply voltage is tabulated in table 3.

The table indicates 3 different supply voltages that will be required: $3.3\,\mathrm{V}$, $5\,\mathrm{V}$ and $12\,\mathrm{V}$. This is achieved by using a $5\,\mathrm{V}$ and $3.3\,\mathrm{V}$ linear voltage regulators and the $12\,\mathrm{V}$ is supply by a external source.
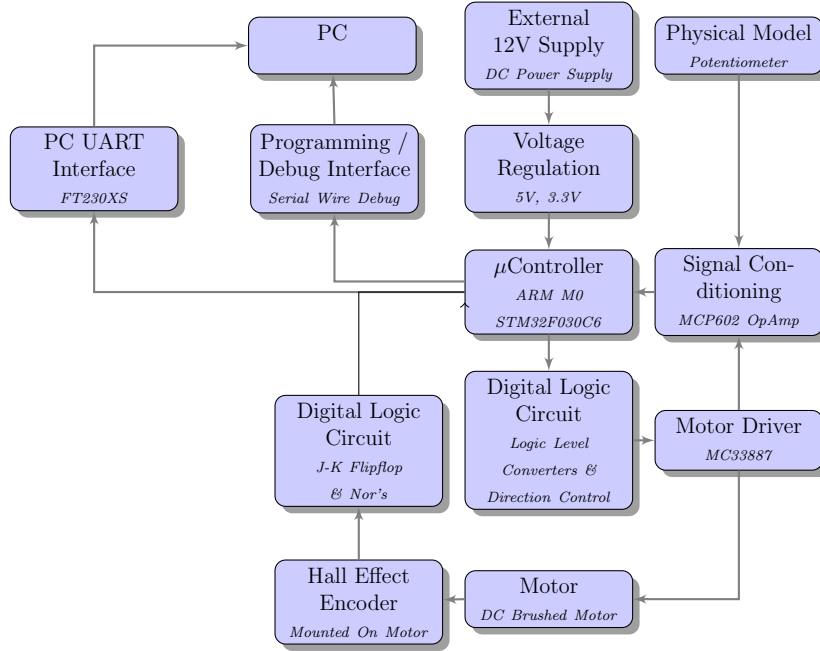
Figure 6: Electronic System Overview

The schematic for each voltage regulator is shown in Appendix XX, where each voltage regulator circuit includes a Light Emitting Diode (LED) to ensure the minimum load is met for each regulator. The LED also acts as a visual debugging method.

11.3 Programming / Debug Interface

11.4 PC UART Interface

The purpose of the UART to serial communication is for data acquisition of the system response and for debugging purposes. The data being sent follows a structure to ensure the reliability of the data. Figure (ref) shows the format of the data being sent.

The data being sent across the UART to serial circuit is retrieved by a computer executing a Python script, listening for any activity on the computer's driver ports and writing the data into a comma-separated value (csv) file that can later be use to analyse the data.

The UART to serial circuit has been tested by doing a loopback test and using a digital logic analyser to verify the data being sent. The loopback test consist of connecting the Tx and Rx lines together and forcefully echo what has been sent to the circuit to be sent back. Figure (ref) in Appendix XXX

16

shows the digital signals sent and received and confirms the working of the UART to Serial circuit.

11.5 Signal Conditioning

The analog signals from the various components is received that will be conditioned to interface with the micro-controller Analog-to-Digital Converter (ADC) to interpret the signal.

The signal from the potentiometer that provides measurements about the angle of the shaft varies between 0-5V. This signal is sent through a simple resistive voltage divider circuit to scale the signal between 0-3V.

The scaled voltage is sent through a unity gain rail-to-rail amplifier, where the mirrored output signal is fed into the ADC. The unity gain amplifier has the characteristic of a high input impedance and low output impedance. The type of ADC used in the STM32F030XX is a successive approximation register (SAR), [8]. The SAR ADC's contains internal capacitor that has suffers from the effect of being depleted if the sampling period is to high. The low impendance from the unity gain amplifier reduces the risk of depleting this internal capacitor because of the low current being pulled.

The current feedback signal that is provided from the motor drive IC varies between 0 and 3V fed into the unity gain operation amplifier. This is done for the same reasons discussed above.

The chosen operational amplifier is the MCP602.

11.6 Motor Driver

The motor driver IC is responsible for directional and rotational control of the brushed DC motor. The motor driver is the MC33887 and contains 2 half H-bridges that controls the direction and speed of the motor. The 2 H-half bridges form a full H-bridge which are Pulse-Width-Modulated(PWM) to control the speed of the motor. The PWM- and direction signal originates from the micro-controller.

The MC33887 provides a proportional current of 1/375 of the current flowing through the high-side of the full H-bridge(reference). This current is sent through resistor of $150\,\Omega$ to provide a voltage signal to represent the current.

The MC33887 is capable of providing up to 6A of continuous current to the motor, while withstanding the high current transients due to the fast switching of a inductive load (ref). The motor driver IC is able to provide the motor with the 12V DC which is externally provided by a DC power supply.

The schematic of supporting passive components to allow the motor driver IC to work is shown in Appendix XXX.

11.7   AND Digital Logic Circuit

The digital logic circuit is responsible for interfacing between the microcontroller and the motor driver IC, and providing the motor driver with the correct PWM signal.

The microcontroller is only able to provide a logical high and low by representing it as a $3.3\,\text{V}$ and $0\,\text{V}$ respectively. The motor driver IC's minimum threshold for a logical high is 3.5V [9]. Thus it is required to use a logic level converter circuit to interface between the 2 devices. This is accomplished using the BSS138 transistor in the circuit diagram shown in Figure 7.

$V_{SS}=5\text{V}$

R_1

Output $\in [5; 0]$

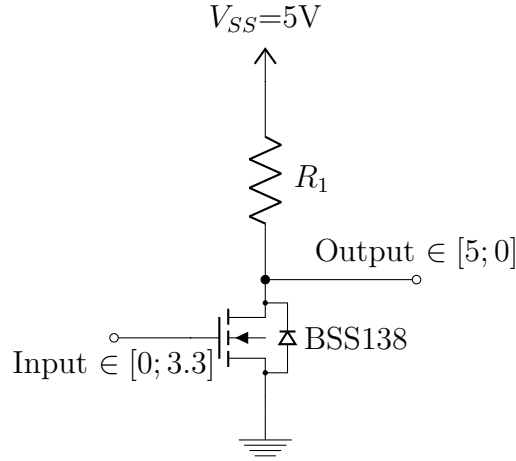Input $\in [0; 3.3]$ BSS138

Figure 7: Logic Level Converter & Inverter Circuit

This identical circuit shown in Figure 7 is a inverter and combining the 2 inputs from the microcontroller, the PWM-signal and directional signal with the inverter and AND-gates the motor speed and direction can be controlled.

Figure **??** shows the overview of the system

11.8   JK FlipFlop's Digital Logic Circuit

The motor hall sensor incremental encoder produces 2 digital signals that has a 90 degree phase between each other shown in Figure (ref). This signal will be read by the microcontroller using interrupts when a rising edge is present. The amount of servicing of theses signals can be reduced by using a J-K Flipflop and NOR logic gates circuit shown in Figure 8.
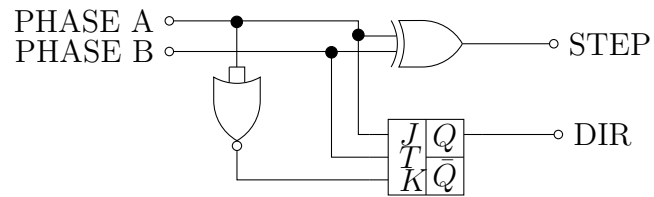
Figure 8: Digital Logic Circuit containing JK-Flipflops, XOR- and NOR Gates

This circuit produces 2 output signals. The first signal will be a logical high or low indicating a change in rotation. The other signal will be a square wave, where each rising edge indicate a incremental rotation of the shaft.

11.9 Microcontroller

12 Verification of Model

References

[1] R. Tedrake. Underactuated robotics: Algorithms for walking, running, swimming, flying, and manipulation (course notes for mit 6.832). [Online]. Available: http://underactuated.mit.edu/

[2] "A case study in approximate linearization: The acrobat example," *Proc. American Control Conference*, 1990.

[3] "The swing up control problem for the acrobat," *IEEE Control Systems*, vol. 47, no. 10, pp. 50–55, 1995.

[4] "An explicit description of null controllable regions of linear systems with saturating actuators," *Systems & Control Letters*, vol. 47, no. 10, pp. 65–78, 2002.

[5] e. a. Gene F. Franklin, J. David Powell, *Feedback Control of Dynamic Systems*, 7th ed. Edingburgh Gate, Harlow, Essex CM20 2JE, England: Pearson Education Limited, 2015.

[6] "On stabilization of an inverted double pendulum with one control torque," *Journal of Compute and Systems Science International*, vol. 45, no. 3, pp. 337–334, 2006.

[7] M. Morzfeld, "The transformation of second-order linear systems into independent equations," Ph.D. dissertation, University of California, Berkeley, 2011.

[8] *How to get the best ADC accuracy in the STM32 microcontrollers*, AN2834 Application note, ST Electronics, 2017.

[9] *5.0 A H-Bridge woth Load Current Feeback*, 12th ed., Freescale Semiconductor, 2 2007, document Number: MC33887.

Appendices

A   Derivation of the Double Pendulum

$$x_1 = l_1 \cos(\theta)$$

$$y_1 = -l_1 \sin(\theta)$$

$$x_2 = L_1 \sin(\theta) + l_2 \sin(\theta + \phi)$$

$$y_2 = -L_1 \cos(\theta) - l_2 \cos(\theta + \phi)$$

$$\dot{x}_2 = L_1 \cos(\theta)\dot{\theta} - l_2 \cos(\theta + \phi)(\dot{\theta} + \dot{\phi})$$

$$\dot{y}_2 = L_1 \sin(\theta)\dot{\theta} + l_2 \sin(\theta + \phi)(\dot{\theta} + \dot{\phi})$$

$$\dot{x}_2^2 = L_1^2 \cos(\theta)^2 \dot{\theta}^2 + l_2^2 \cos(\theta + \phi)^2 (\dot{\theta} + \dot{\phi})^2 + 2L_1 l_2 \dot{\theta}(\dot{\theta} + \dot{\theta}) \cos(\theta) \cos(\theta + \phi)$$

$$\dot{y}_2^2 = L_1^2 \sin(\theta)^2 \dot{\theta}^2 + l_2^2 \sin(\theta + \phi)^2 (\dot{\theta} + \dot{\phi})^2 + 2L_1 l_2 \dot{\theta}(\dot{\theta} + \dot{\theta}) \sin(\theta) \sin(\theta + \phi)$$

$$\dot{x}_2^2 + \dot{y}_2^2 = L_1^2 \dot{\theta}^2 [\cos(\theta)^2 + \sin(\theta)^2] + l_2^2 (\dot{\theta} + \dot{\phi})^2 [\cos(\theta + \phi)^2 + \sin(\theta + \phi)^2] +$$

$$2L_1 l_2 \dot{\theta}(\dot{\theta} + \dot{\phi})[\cos(\theta) \cos(\theta + \phi) + \sin(\theta) \sin(\theta + \phi)]$$

Using the following trigonometric identities

$$\cos(\gamma)^2 + \sin(\gamma)^2 = 1$$

$$\cos(\gamma) \cos(\alpha) + \sin(\gamma) \sin(\alpha) = \cos(\gamma - \alpha)$$

the above equation resolves to:

$$V_2^2 = L_1 \dot{\theta}^2 + l_2^2 (\dot{\theta} + \dot{\phi})^2 + 2L_1 l_2 (\dot{\theta} + \dot{\phi})\dot{\theta} \cos(\phi)$$

The kinetic energy in the system consist of the fixed rotation of the underactuated pendulum and the rotation and velocity of the actuated pendulum.

$$T = \frac{1}{2} I_A \dot{\theta}^2 + \frac{1}{2} I_B (\dot{\theta} + \dot{\phi})^2 + \frac{1}{2} m_2 V_2^2$$

$$T = \frac{1}{2} I_A \dot{\theta}^2 + \frac{1}{2} I_B (\dot{\theta} + \dot{\phi})^2 + \frac{1}{2} m_2 [L_1 \dot{\theta}^2 + l_2^2 (\dot{\theta} + \dot{\phi})^2 + 2L_1 l_2 (\dot{\theta} + \dot{\phi})\dot{\theta} \cos(\phi)]^2$$

The potential energy in the system is defined as

$$V = -m_1 g l_1 \cos(\theta) - m_2 g [L_1 \cos(\theta) + l_2 \cos(\theta + \phi)]$$

The Lagrange is defined as

$$\mathcal{L} = T - V$$

$$\mathcal{L} = \frac{1}{2} I_A \dot{\theta}^2 + \frac{1}{2} I_B (\dot{\theta} + \dot{\phi})^2 + \frac{1}{2} m_2 [L_1 \dot{\theta}^2 + l_2^2 (\dot{\theta} + \dot{\phi})^2 + 2 L_1 l_2 (\dot{\theta} + \dot{\phi}) \dot{\theta} \cos(\phi)]^2 + m_1 g l_1 \cos(\theta) +$$

$$m_2 g [L_1 \cos(\theta) + l_2 \cos(\theta + \phi)]$$

$$\frac{\partial \mathcal{L}}{\partial \theta} = -m_1 g l_1 \sin(\theta) - m_2 g L_2 \sin(\theta) - m_2 g l_2 \sin(\theta + \phi)$$

$$\frac{d}{dt} \frac{\partial \mathcal{L}}{\partial \dot{\theta}} = I_A \ddot{\theta} + I_B \ddot{\theta} + I_B \ddot{\phi} + m_2 L_1^2 \ddot{\theta} + m_2 l_2^2 \ddot{\theta} + m_2 l_2^2 \ddot{\phi} + 2 m_2 L_1 l 2 \ddot{\theta} \cos(\phi) - 2 m_2 L_1 l_2 \dot{\theta} \dot{\phi} \sin(\phi) +$$

$$m_2 L_1 l_2 \ddot{\phi} \cos(\phi) - m_2 L_1 l_2 \dot{\phi}^2 \sin(\phi)$$

$$\frac{\partial \mathcal{L}}{\partial \phi} = -m_2 L_1 l_2 (\dot{\theta} + \dot{\phi}) \dot{\theta} \sin(\phi) - m_2 g l_2 \sin(\theta + \phi)$$

$$\frac{d}{dt} \frac{\partial \mathcal{L}}{\partial \dot{\phi}} = I_B \ddot{\theta} + I_B \ddot{\phi} + m_2 l_2^2 \ddot{\theta} + m_2 l_2^2 \ddot{\phi} + m_2 L_1 l_2 \ddot{\theta} \cos(\phi) - m_2 L_1 l_2 \dot{\theta} \dot{\phi} \sin(\phi)$$

The differential equation describing the dynamics of the system is

$$\frac{d}{dt} \frac{\partial \mathcal{L}}{\partial \vec{\dot{q}}} - \frac{\partial \mathcal{L}}{\partial q} = B(\dot{q}) + \tau(q)$$

where $q = \begin{bmatrix} \theta \\ \phi \end{bmatrix}$

B   Linearisation of the Double Pendulum

The system will be linearised using the Taylor Series Expansion around the operating point

$$\vec{Q}_s = [\vec{q}_s, \dot{\vec{q}}_s, \ddot{\vec{q}}_s]^T = [\pi, 0, 0, 0, 0, 0]$$

and approximate the system as

$$F([\vec{q}, \dot{\vec{q}}, \ddot{\vec{q}}]^T) = F(\vec{Q}) \approx F(\vec{Q}_s) + [\Delta \vec{Q} \cdot \nabla F(\vec{Q}_s)]$$

where $\Delta \vec{Q} = \vec{Q} - \vec{Q}_s$. Resulting in 2 linear dependent equations:

$$\Delta\ddot{\theta}(I_A + I_B + m_2 l_2^2 + m_2 L_1^2 + 2m_2 l_2 L_1) + \Delta\ddot{\phi}(I_B + m_2 l_2^2 + m_2 L_1 l_2) +$$
$$\Delta\theta(-m_1 g l_1 - m_2 g L_1 - m_2 g l_2) + \Delta\phi(-m_2 g l_2) = \Delta\dot{\theta} b_1 \quad (1)$$

$$\Delta\ddot{\theta}(I_B + m_2 l_2^2 + m_2 L_1 l_2) + \Delta\ddot{\phi}(I_B + m_2 l_2^2) + \Delta\theta(-m_2 g l_2) +$$
$$\Delta\phi(-m_2 g l_2) = \tau + (\Delta\dot{\theta} + \Delta\dot{\phi}) b_2 \quad (2)$$

Equation (1) and (2) can be rewritten in state-space form by substituting the 2 equations into each other to remove the angular acceleration term of the other respectable angle.

The state space variables are chosen as Δq and $\Delta \dot{q}$ which results in the state space representation as:

$$\begin{bmatrix} \Delta\dot{\theta} \\ \Delta\dot{\phi} \\ \Delta\ddot{\theta} \\ \Delta\ddot{\phi} \end{bmatrix} = \begin{bmatrix} x & x & x & x \\ x & x & x & x \\ 0 & 0 & 1 & 0 \\ 0 & 0 & 0 & 1 \end{bmatrix} \begin{bmatrix} \Delta\theta \\ \Delta\phi \\ \Delta\dot{\theta} \\ \Delta\dot{\phi} \end{bmatrix} + \begin{bmatrix} 0 \\ 1 \\ 0 \\ 0 \end{bmatrix} \tau$$

$$\begin{bmatrix} \Delta\theta \\ \Delta\phi \\ \Delta\dot{\theta} \\ \Delta\dot{\phi} \end{bmatrix} = \begin{bmatrix} 1 & 0 & 0 & 0 \\ 0 & 1 & 0 & 0 \\ 0 & 0 & 1 & 0 \\ 0 & 0 & 0 & 1 \end{bmatrix} \begin{bmatrix} \Delta\theta \\ \Delta\phi \\ \Delta\dot{\theta} \\ \Delta\dot{\phi} \end{bmatrix} + [0]\, \tau$$

The compact form will be used as

$$\dot{\vec{x}} = \boldsymbol{A}\vec{x} + \boldsymbol{B}\vec{u}$$

and

$$\vec{y} = \boldsymbol{D}\vec{x} + \boldsymbol{0}\vec{u}$$

C De-coupling of the Linearised System into 2 Independent Equations

D Collocated Linearisation

E   Proof of Pumping Energy into System